

# FORMATION MECHANISM OF $\text{YFeO}_3$ NANOPARTICLES UNDER THE HYDROTHERMAL CONDITIONS

V. I. Popkov<sup>1,3</sup>, O. V. Almjashaeva<sup>2,3</sup>

<sup>1</sup>Saint Petersburg State Technological Institute (Technical University), St. Petersburg, Russia

<sup>2</sup>Saint Petersburg Electrotechnical University 'LETI', St. Petersburg, Russia

<sup>3</sup>Ioffe Physical Technical Institute, St. Petersburg, Russia

vadim.i.popkov@gmail.com, almjashaeva@mail.ru

**PACS 61.46.+w**

Yttrium orthoferrite nanocrystals with an average crystallite size of 55 – 60 nm have been obtained under hydrothermal conditions. The influence of the hydrothermal synthesis temperature on the structure and crystallite size has been investigated. Mechanism of the  $\text{YFeO}_3$  formation under the hydrothermal conditions has been proposed.

**Keywords:** yttrium orthoferrite,  $\text{YFeO}_3$ , hydrothermal synthesis, phase formation, formation mechanism.

*Received: 1 July 2014*

*Revised: 4 September 2014*

## 1. Introduction

Nanoparticles are often synthesized by 'soft-chemical' methods because the techniques are accessible, simple, use relatively low temperatures and have a large number of varied parameters that allow one to control products' properties [1–4]. Additionally, these methods usually allow relatively rapid forming of nanoparticles [5]. One such method is hydrothermal synthesis, which permits to one to obtain relatively non-agglomerated oxide nanoparticles with a narrow size distribution [6–11].

The solid state method is conventionally used to obtain yttrium orthoferrite. In this case, mechanically mixed oxides of the corresponding metals [12] or a mixture of its hydroxides obtained by the coprecipitation process can be used as precursors [13, 14]. However, the process can be complicated by yttrium orthoferrite thermodynamic instability and yttrium-iron garnet  $\text{Y}_3\text{Fe}_5\text{O}_{12}$  formation at high temperatures [15]. Additionally, the obtained nanoparticles are highly agglomerated and their size is relatively large. Therefore, investigation of  $\text{YFeO}_3$  formation under hydrothermal synthesis conditions is of interest. It should be noted, that despite the potential for using this method in nanoparticle synthesis, data about its application for  $\text{YFeO}_3$  synthesis is very limited. In works [18, 19], the authors use concentrated KOH solution as mineralizer to reduce the synthesis temperature. This resulted in yttrium orthoferrite formation [18] as well as in formation of the almost all rare-earth metals orthoferrites [19], but the obtained nanoparticle sizes were 10 – 30  $\mu\text{m}$ . This is due to partial dissolution of the initial hydroxides under hydrothermal conditions in the presence of the concentrated KOH solution, so that rare-earth orthoferrite formation is carried out by crystallization from solution, leading to rapid nanoparticle growth.

Another variant of hydrothermal synthesis usage is described elsewhere [20]. In this case, hydrothermal processing was used only for precursor preparation – hydrolysis of yttrium and iron nitrate mixture was carried out under hydrothermal conditions at 200 °C. The obtained X-ray amorphous sample was heat treated in air from 400 – 1000 °C. The formation of yttrium

orthoferrite nanoparticles with average size of  $\sim 100$  nm was observed at  $800$  °C, which corresponds to temperature of the  $YFeO_3$  formation from coprecipitated hydroxides under thermal treatment [14,21].

Thus, investigation of the possibility and the mechanism by which weakly agglomerated yttrium orthoferrite nanoparticles are formed under hydrothermal conditions is of great interest.

## 2. Experimental

### 2.1. Synthesis procedure

An yttrium and iron hydroxide mixture was obtained using the reprecipitation process. An  $Y(NO_3)_3$  and  $Fe(NO_3)_3$  solution mixture was added in a dropwise manner to 1 M NaOH solution under vigorous stirring. The obtained precipitate was washed with distilled water and dried at  $70$  °C.

Hydrothermal treatment was then carried out according to the procedure described in [11] at  $200 - 400$  °C, at the 50 MPa over 3 hours. Distilled water was used as the solvent.

### 2.2. Characterization of the prepared samples

The elemental composition of the specimens were analyzed by means of scanning electron microscopy (SEM) using Hitachi S-570, coupled with Oxford Link Pentafet microprobe analyzer.

The phase composition of the specimens were controlled by powder X-ray diffraction (XRD) using a Shimadzu XRD-700 with monochromatic  $CuK_{\alpha}$  radiation ( $\lambda=0.154051$  nm). Qualitative X-Ray analysis was carried out with powder base of the diffraction data PDF2-2012 using, quantitative X-Ray analysis was carried out with using of the Rietveld method [22]. Average crystallite size was calculated according to Scherer's equation [23].

## 3. Results and discussion

According to the results of phase composition analysis obtained after coprecipitation, the material is X-ray amorphous. Results of elemental analysis showed that molar ratio of Fe:Y was 50.4:49.6 and corresponded to the stoichiometric value within the range of experimental error.

According to the results of X-ray analysis (Fig. 1), hydrothermal treatment at  $200$  °C leads to iron (III) oxide-hydroxide  $FeOOH$  (goethite) crystallization only. With an increase in the treatment temperature to  $250$  °C, a reduction in the peak intensity was observed as well as the appearance of weak peaks of iron (III) oxide  $Fe_2O_3$  (hematite), yttrium hydroxycarbonate  $Y_2(OH)_4CO_3$ , and yttrium orthoferrite  $YFeO_3$ . Further increase of the hydrothermal synthesis temperature leads to goethite peak disappearance (at  $350$  °C) and to  $YFeO_3$  peaks intensity growth while  $Fe_2O_3$  and  $Y_2(OH)_4CO_3$  peak intensities were practically unchanged.

The presence of yttrium hydroxycarbonate can be explained by the high reactivity of the newly-precipitated yttrium hydroxide, which leads to its quick reaction with atmospheric carbon dioxide [24,25].

The presence of the goethite reflection at  $Fe_2O_3$ -stable temperatures [23,24] can be explained as a result of an iron (III) oxide reverse hydration process that may be caused due to autoclave cooling inertia. So, it would seem that  $FeO(OH)$  doesn't participate in yttrium orthoferrite formation.

Quantitative X-ray analysis results are shown in Fig. 2. The content of  $FeO(OH)$  and  $Fe_2O_3$  is represented in terms of  $FeO_{1.5}$ , and analogically content of  $Y_2(OH)_4CO_3$  – in terms of  $YO_{1.5}$ .

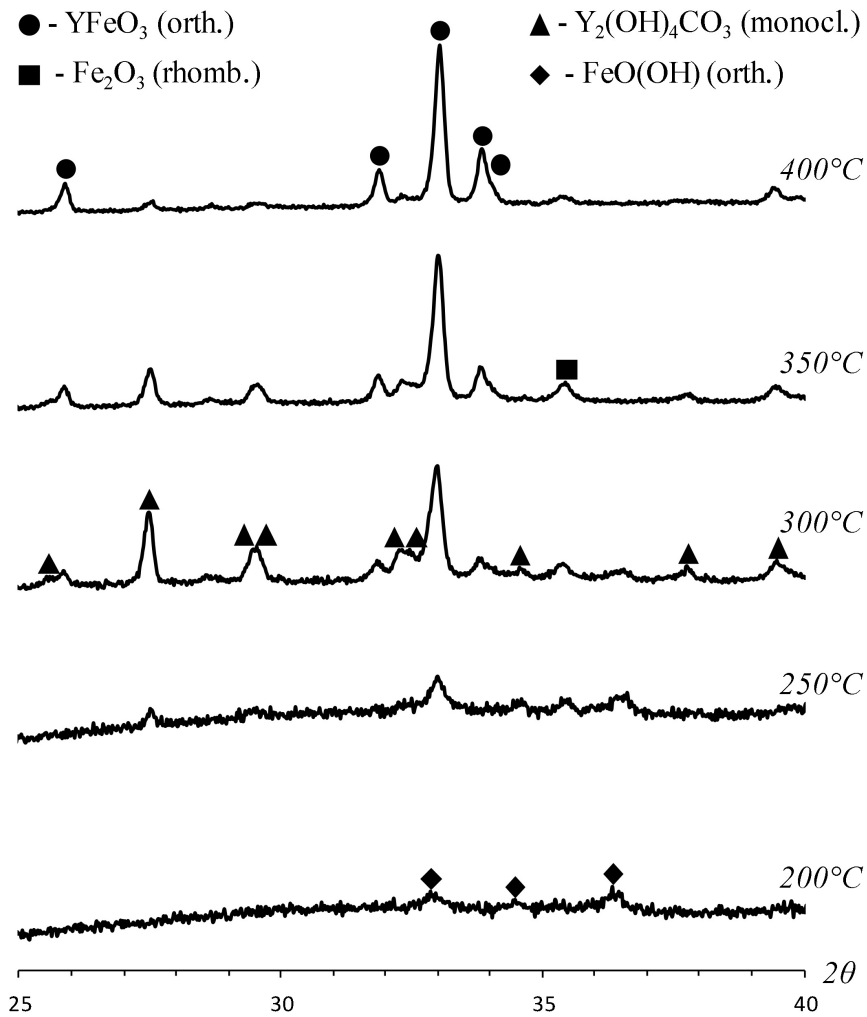


FIG. 1. X-ray diffractograms of the hydrothermal synthesis products

Analysis of the data Fig. 2 indicates that initial components may exist in two essentially different states.

Hydroxycarbonate formation leads to precursor inhomogeneity and to the separated crystallization of the iron-containing and yttrium-containing components. At the same time, the homogeneous precursor portion remains X-ray amorphous during hydrothermal treatment and gradually transforms into yttrium orthoferrite without intermediate phase crystallization. This system behavior may be connected with existence of the relatively stable nanoheterogeneous structures. One can imagine such structure like a nanoscale amorphous clusters of the iron-containing and yttrium-containing precipitate components.

Average crystallite size was calculated from X-ray line broadening for each phase. Obtained data are shown in Fig. 3. Yttrium-containing phase crystallite size is given in terms of yttrium oxide with using molar volume of the  $Y_2(OH)_4CO_3$  (monoclinic) and  $Y_2O_3$  (cubic).

Comparison of data in Fig. 2 and 3 allows one to assume that under hydrothermal conditions, nanoparticle formation occurs from amorphous clusters as described above. These clusters transform into  $Fe_2O_3$  and  $Y_2O_3$  crystallites, or they can aggregate in tetrahedral complexes to subsequently form  $YFeO_3$  nanoparticles. The proposed mechanism for  $YFeO_3$  nanoparticle formation is shown schematically in Fig. 4.

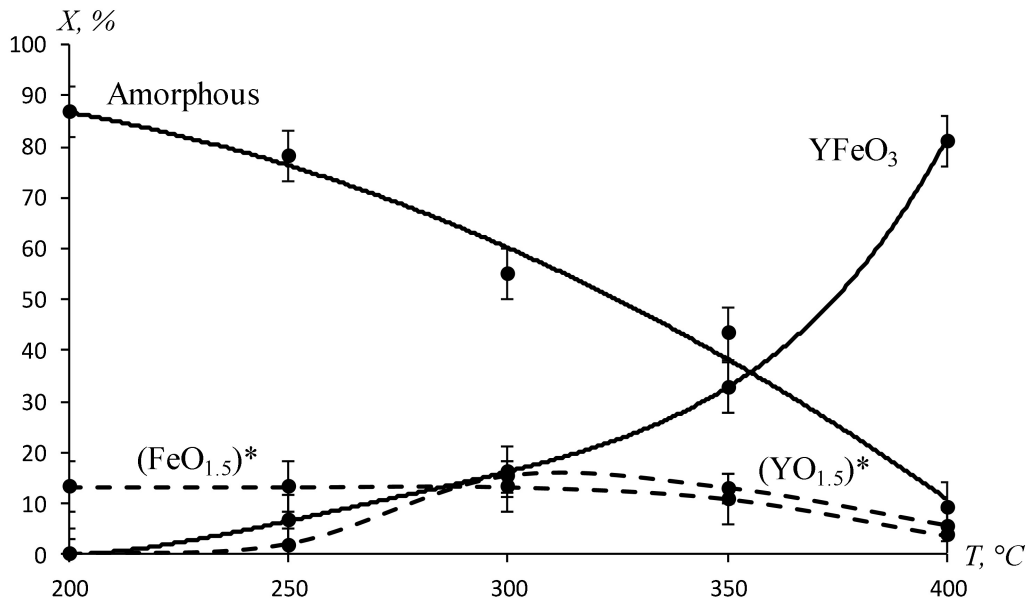


FIG. 2. Molar fraction ( $X$ , %) depending on the isothermal exposure temperature ( $T$  °C)

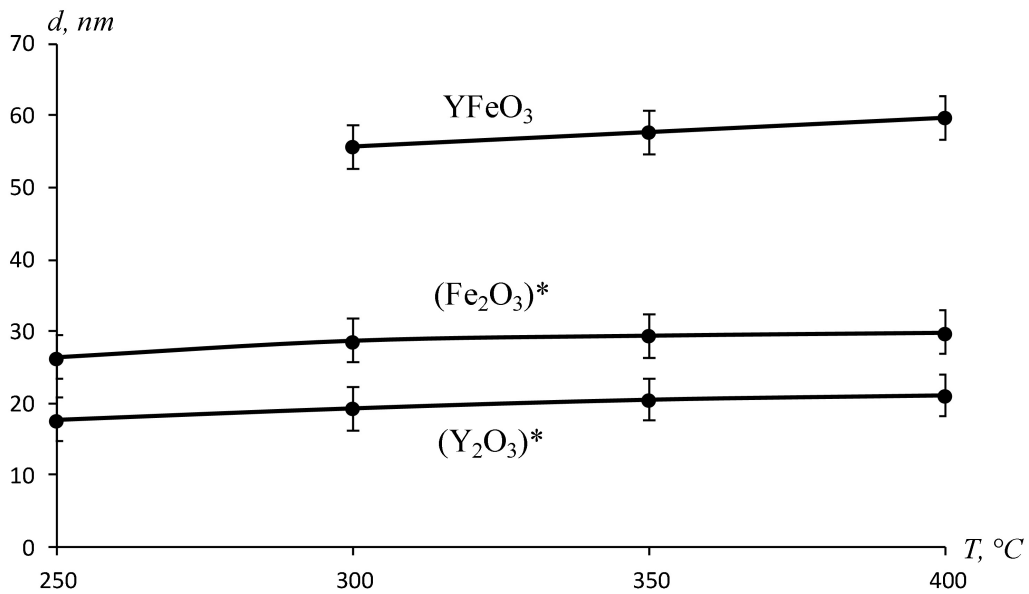


FIG. 3. Average crystallite size ( $d$ , nm) depending on the isothermal exposure temperature ( $T$  °C)

It should be noted that this assumption can be confirmed by crystallite size comparison of simple oxides and  $\text{YFeO}_3$ .

#### 4. Conclusion

Orthorhombic yttrium orthoferrite with average crystallite size from  $55 \pm 3$  nm to  $60 \pm 3$  nm was obtained by hydrothermal treatment of the coprecipitated iron (III) and yttrium hydroxides. It was shown that  $\text{YFeO}_3$  formation proceeded from four-fold complexes of the

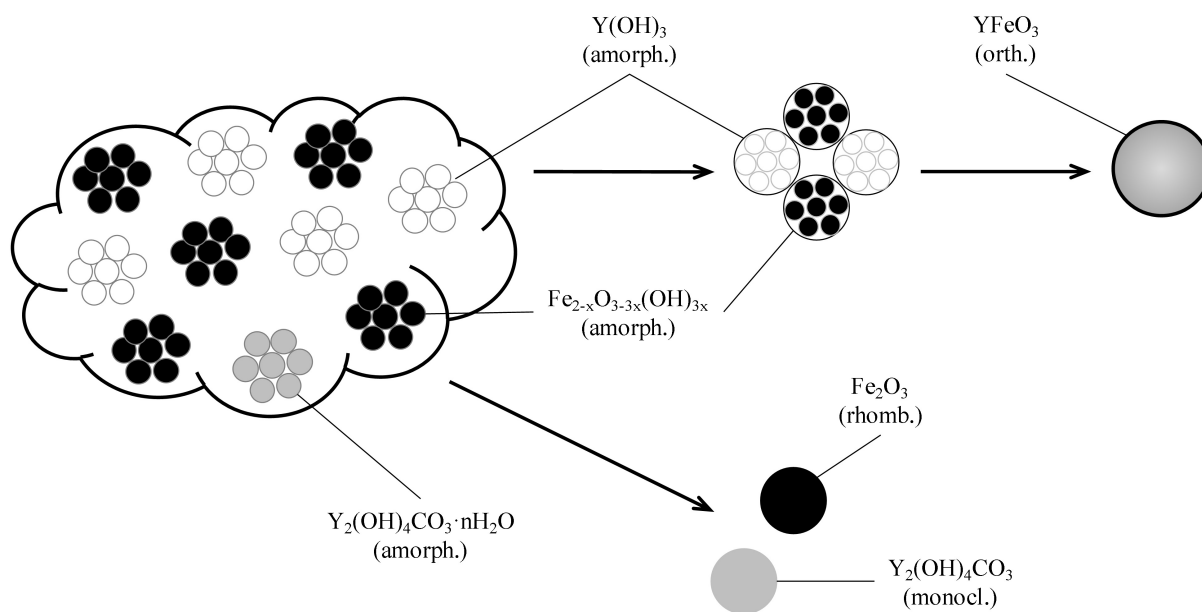


FIG. 4. Formation mechanism of  $YFeO_3$  under the hydrothermal conditions

iron-containing and yttrium-containing amorphous clusters that resulted in the formation of relatively large yttrium orthoferrite nanoparticles. The presence of iron (III) oxide and yttrium hydroxycarbonate may be associated with exposure to atmospheric carbon dioxide, which occurs in the precipitation stage. Therefore, iron-containing and yttrium-containing phase crystallization occurs independently of the main  $YFeO_3$  formation process.

### Acknowledgments

The authors would like to thank Prof. V. V. Gusarov for interest in the work and help in the interpretation of results.

The authors wish to thank V. S. Fundamensky for help in complex X-ray analysis and interpretation of its results.

This work was financially supported by the Russian Foundation for Basic Research (project 13-03-12470).

### References

- [1] Livage J. Vanadium pentoxide gels. *Chemistry of Materials*, **3** (4), P. 578 (1991).
- [2] Sanchez C., Rozes L., et al. "Chimie douce": A land of opportunities for the designed construction of functional inorganic and hybrid organic-inorganic nanomaterials. *Comptes Rendus Chimie*, **13** 3 (2010).
- [3] Brec R., Rouxel J., Tournoux M. Soft chemistry routes to new materials: chimie douce. Proceedings of the international symposium held in Nantes, France, September 6–10, 1993, Aedermannsdorf, Switzerland: Trans Tech Pubs, (1994).
- [4] Gopalakrishnan J. Chimie Douce Approaches to the Synthesis of Metastable Oxide Materials. *Chemistry of Materials*, **7** (7), P. 1265 (1995).
- [5] Gusarov V.V. Fast solid phase chemical reactions. *Zhurnal Obshchei Khimii*, **67** (12), P. 1959–1964 (1997).
- [6] Pozhidaeva O.V., Korytkova E.N., Drozdova I.A., Gusarov V.V. Phase state and particle size of ultradispersed zirconium dioxide as influenced by conditions of hydrothermal synthesis. *Russ. J. Gen. Chem.*, **69** (8), P. 1265–1269 (1999).
- [7] Pozhidaeva O.V., Korytkova E.N., Romanov D.P., Gusarov V.V. Formation of  $ZrO_2$  nanocrystals in hydrothermal Media of various chemical compositions. *Russ. J. Gen. Chem.*, **72** (6), P. 910–914 (2002).

- [8] Al'myasheva O.V., Korytkova E.N., Maslov A.V., Gusarov V.V. Preparation of nanocrystalline alumina under hydrothermal conditions. *Inorg. Mater.*, **41** (5), P. 460–467 (2005).
- [9] Komlev A.A., Gusarov V.V. Mechanism of the nanocrystals formation of the spinel structure in the MgO–Al<sub>2</sub>O<sub>3</sub>–H<sub>2</sub>O system under the hydrothermal conditions. *Russ. J. Gen. Chem.*, **81** (11), P. 2222–2230 (2011).
- [10] Vasilevskaya A.K., Almjashaeva O.V. Features of phase formation in the ZrO<sub>2</sub>–TiO<sub>2</sub> system under hydrothermal conditions. *Nanosystems: physics, chemistry, mathematics*, **3** (4), P. 75–81 (2012).
- [11] Tugova E.A., Zvereva I.A. Formation mechanism of GdFeO<sub>3</sub> nanoparticles under the hydrothermal conditions. *Nanosystems: physics, chemistry, mathematics*, **4** (6), P. 851–856 (2013).
- [12] Nakayama S. LaFeO<sub>3</sub> perovskite-type oxide prepared by oxide-mixing, co-precipitation and complex synthesis methods. *J. Mater. Sci.*, **6**, P. 5643–5648 (2001).
- [13] Tac D.V., Mittova V.O., Almjashaeva O.V., Mittova I.Ya. Synthesis, structure, and magnetic properties of nanocrystalline Y<sub>3–x</sub>La<sub>x</sub>Fe<sub>5</sub>O<sub>12</sub> (0 ≤ x ≤ 0.6). *Inorg. Mater.*, **48** (1), P. 74–78 (2011).
- [14] Tac D.V., Mittova V.O., Almjashaeva O.V., Mittova I.Ya. Synthesis and magnetic properties of nanocrystalline Y<sub>1–x</sub>Cd<sub>x</sub>FeO<sub>3–δ</sub> (0 ≤ x ≤ 0.2). *Inorg. Mater.*, **47** (10), P. 1141–1146 (2011).
- [15] Tang P., Chen H., Cao F., Pan G. Magnetically recoverable and visible-light-driven nanocrystalline YFeO<sub>3</sub> photocatalysts. *Catal. Sci. Technol.*, **1** (7), P. 1145–1148 (2011).
- [16] Tien N.A., Mittova I.Ya., et al. lanthanum orthoferrite. *Glas. Phys. Chem.*, **34** (6), P. 756–761 (2008).
- [17] Tien N.A., Mittova I.Ya., Al'myasheva O.V. Influence of the synthesis conditions on the particle size and morphology of yttrium orthoferrite obtained from aqueous solutions. *Russ. J. Appl. Chem.*, **82** (11), P. 1915–1918 (2009).
- [18] Shang M., Zhang C., et al. The multiferroic perovskite YFeO<sub>3</sub>. *Appl. Phys. Lett.*, **102** (6), P. 062903(3 p.) (2013).
- [19] Zhou Z., Guo L., et al. Hydrothermal synthesis and magnetic properties of multiferroic rare-earth orthoferrites. *J. Alloys Compd. Elsevier B*, **583**, P. 21–31 (2014).
- [20] Tang P., Sun H., Chen H., Cao F. Hydrothermal processing-assisted synthesis of nanocrystalline YFeO<sub>3</sub> and its visible-light photocatalytic activity. *Curr. Nanosci.*, **8**, P. 64–67 (2012).
- [21] Tien N.A., Almjashaeva O.V., et al. Synthesis and magnetic properties of YFeO<sub>3</sub> nanocrystals. *Inorg. Mater.*, **45** (11), P. 1304–1308 (2009).
- [22] Rietveld H.M. A profile refinement method for nuclear and magnetic structures. *J. Appl. Crystallogr.*, **2** (2), P. 65–71 (1969).
- [23] Patterson A. The Scherrer formula for X-ray particle size determination. *Phys. Rev.*, **56**, P. 978–982 (1939).
- [24] Christensen A.N., Hazell R.G. Hydrothermal investigation of the systems Y<sub>2</sub>O<sub>3</sub>–H<sub>2</sub>O–Na<sub>2</sub>O, Y<sub>2</sub>O<sub>3</sub>–D<sub>2</sub>O–Na<sub>2</sub>O, Y<sub>2</sub>O<sub>3</sub>–H<sub>2</sub>O, and Y<sub>2</sub>O<sub>3</sub>–H<sub>2</sub>O–NH<sub>3</sub>. The crystal structure of Y(OH)<sub>3</sub>. *Acta Chem. Scand.*, **21**, P. 481–492 (1967).
- [25] Christensen A.N., Hazell R.G. The crystal structure of Ho<sub>2</sub>(OH)<sub>4</sub>CO<sub>3</sub>. *Acta Chem. Scand.*, **38** (A), P. 157–161 (1984).